



Advanced Virgo Squeezer Technical Design Report

VIR-xxxA-12

Issue 1

Magari Mettiamo la lista

October 7, 2014

Contents

1		1
2		3
3	OPO Pump Beam	5
3.1	Pump Beam Source: the choice of an home-made Second Harmonic Generator . . .	5
3.2	Homemade SHG	6
3.2.1	SHG optical design	6
3.2.2	Temperature control	8
3.2.3	Mechanics	8
3.2.4	PDH locking system for the SHG	9
3.2.5	IR to GREEN conversion	10
3.3	Pump Beam Power Stabilization	11
3.3.1	System description	12
3.3.2	Mechanical design	13
3.3.3	Electronic control loop	13
3.4	OPO pre-Mode Cleaner Cavity	15
3.4.1	532MC optical parameters	15
3.4.2	532MC mechanical design	15
3.4.3	532MC control system	16

Chapter 1

Chapter 2

Chapter 3

OPO Pump Beam

Introduction

3.1 Pump Beam Source: the choice of an home-made Second Harmonic Generator

There are two possibilities to supply the pump beam for the squeezer: the first one is to use a commercial low noise NPRO Nd:YAG frequency duplicated laser, whose second harmonic (SH) field can be used as OPO pump beam, while the fundamental beam can be used for the needed 1064 nm beams (the homodyne local oscillator (LO), the squeezer alignment beam); the second is to build the second harmonic generator (SHG) 'at home', starting by the same kind of commercial low noise NPRO Nd:YAG laser not doubled.

The excellent frequency features of the available commercial doubled Nd:Yag laser (extremely narrow linewidth, very low frequency noise), added to the relative high level of their SH power, (that is enough for the good part of the OPO squeezers, that presently have a typical threshold value for the pump power around 50 mW) and added to their very compact and robust mechanics, render these systems good candidates and, often, preferred solutions as pump source for the OPO based generators of light quantum states []. Moreover from the economical point of view, when considering the possibility to buy a new laser for this kind of apparatus, the difference between the not doubled and the doubled model is often of the order of about 20 keuro, so that for a starting investment, a proclivity for the doubled system could be done when pondered the total costs of a home-made SHG (control electronics included) and when the latest is not yet available in laboratory.

An excellent doubled laser that we have considered is the Prometheus100NE produced by Coherent. This laser belongs to a family of ultra-narrow linewidth (1 kHz), tunable CW lasers available in a single, compact package containing both 532 and 1064 nm wavelengths. It is the same Nd:YAG Mephisto laser (a well known and used system in the Virgo-LIGO collaboration) frequency doubled. It has extraordinary spectral features (both the wavelengths show an extremely low noise (-140 dB/Hz RIN)) and a wide range of tunability (30 GHz and 60 GHz for the fundamental and SH, respectively). The model Prometheus100NE supplies power of 1.5 W at 1064 nm and 100 mW at 532 nm, well above the expected OPO threshold of about **40 mW**. Moreover, respect to its progenitor, the Innolight Diabolo laser, it has a single pass frequency duplication system and not an OPA: this assures more stability and reduces the photo-thermal aging of the SHG non-linear crystal (SH-NLC).

The main disadvantage of the commercial system is that the users have not total control on it in case of damage and malfunction of some parts, (electronics and optics). In particular the replacement of them results more expensive and requires more time, especially if for the reparation is needed the shipment to the manufacturing company. The latest aspect is particularly critical especially in long term operations, like in the case of a squeezing set-up for gravitational wave detector.

From this point of view, an home-made SHG allows more flexibility and it results to be less expensive and, *a regime*, time saving. A spare element can easily made and available. This reasons really seems the stronger argument in favor of it respect the commercial systems, that had led to choose it in the yet operating squeezing sources at GEO600 and LIGO [13, 6, 11, 3]. All the other considerations seem to be not so strong to favor the home-made SHG respect to the Prometheus or Diabolo systems. For example, by literature and by the GEO-LIGO experience are known that the tray light in the whole set-up and the eventual residual IR produced by the SHG are very critical for the squeezer ([10, 11, 3]). The SHG is the principal IR stray light source thanks to the needed relative high infrared pump intensity. Nevertheless, even if it could happen that typically the laser companies do not take into account these issues and do not make use of high quality optics to minimize the scattered and stray light, the latest can be characterized and, if necessary, filtered by means of suitable systems, like dichroic filters along the green path. On the other hand even the home-made SHG requires similar precautions. Moreover in literature and in GEO600 and LIGO themselves there are not a quantifications of this issues that could lead to prefer one system respect to the other.

In conclusion, after these consideration we propose to realize a home-made SHG for the definitive AdV-Virgo squeezer.

3.2 Homemade SHG

The in-cavity second harmonic generation has been used for both the GEO-600 and LIGO squeezers [1, 7]. In both cases the cavity is based on the design developed at the AEI of Hannover [GEO PhD thesis]. We will also start with this design with slight modifications. First we increase the meniscus reflectivity to optimize the conversion efficiency at lower IR power and second in the mechanical design we tried to avoid the use of vacuum grease and conductive paste that should spoil the non linear crystal properties.

3.2.1 SHG optical design

The SHG cavity is a linear cavity with a non linear crystal (NLC) inside. The cavity is designed to be resonant at 1064 nm. The chosen crystal is a $1.00 \times 1.50 \times 9.30 \text{ mm}^3$ PPKTP¹ with 9 μm of poling period which produces the maximum conversion efficiency at about 35 °C [9]. One surface has a radius of curvature (RoC) of 8 mmis HR-coated for both 1064 nm and 532 nm light, the other surface is plano and AR-coated for both wavelengths².

¹We decided to use a periodically poled crystal because of the high conversion efficiency. However it has recently been demonstrated [] that those crystals after prolonged use could be damaged by an intense green field. If we will be affected by this problem, we will move towards the traditional 7% MgO:LiNbO₃ (MgLN).

²

- flat side: $R < 0.1\% @ 1064 \text{ nm}$ & $R < 0.2\% @ 532 \text{ nm}$ at 0 °C
- spherical side: $R > 99.975\% @ 1064 \text{ nm}$ & $@ 532 \text{ nm}$ at 0 °C

The spherical surface of the crystal provides for one mirror of the cavity. The second mirror is a meniscus with a diameter of 12.7 mm. The inner facet has a radius of curvature of 25mm and a power reflectivity of $R_{1064} = 96\%$ and $R_{532} < 2\%$, respectively. The outer facet is AR-coated ($R_{1064} < 0.1\%$ and $R_{532} < 0.2\%$) and has an ROC of 20mm. All values are specified for an angle of incidence (AOI) of 0° . This results in a finesse of $\mathcal{F} \approx 123$ for the fundamental 1064nm field. The meniscus IR reflectivity has been chosen to be optimized at the IR input power of $\approx 200mW$ (see Fig. 3.1).

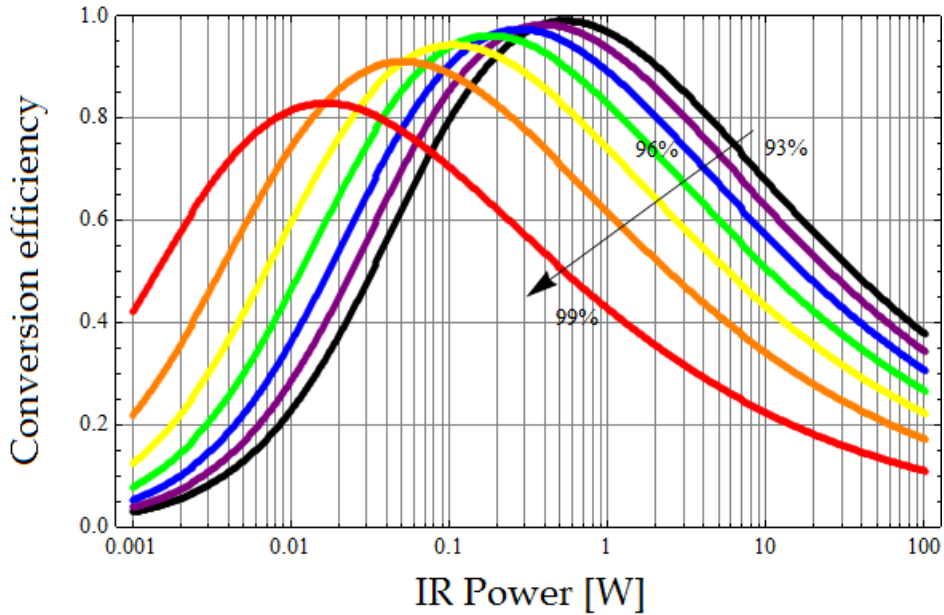


Figure 3.1. Conversion efficiency simulation. The chosen reflectivity (96%) allows a conversion efficiency of 97% with $P_{IR} \approx 200mW$.

The air gap between the meniscus and the plane AR-coated surface of the crystal has to be chosen to operate the cavity in stable configuration. The results of a FINESSE [4] simulation of the cavity stability are shown in Fig. 3.2. For a stable operation, the air gap can extend from 20.0mm to 24.2mm. For the SHG cavity, an air gap of 22mm has been chosen, resulting in an expected beam waist radius of $27.2\mu m$ situated at a distance of 2.8mm from the crystal's AR-coated facet. Taking into account the refractive index of PPKTP at 1064nm, $n = 1.8306$, the optical cavity length is $L = 78mm$, which leads to a linewidth (full width half maximum, FWHM) of $\Delta f_{FWHM} \approx 31.3MHz$ and a free spectral range of $\Delta f_{FSR} \approx 3.84GHz$.

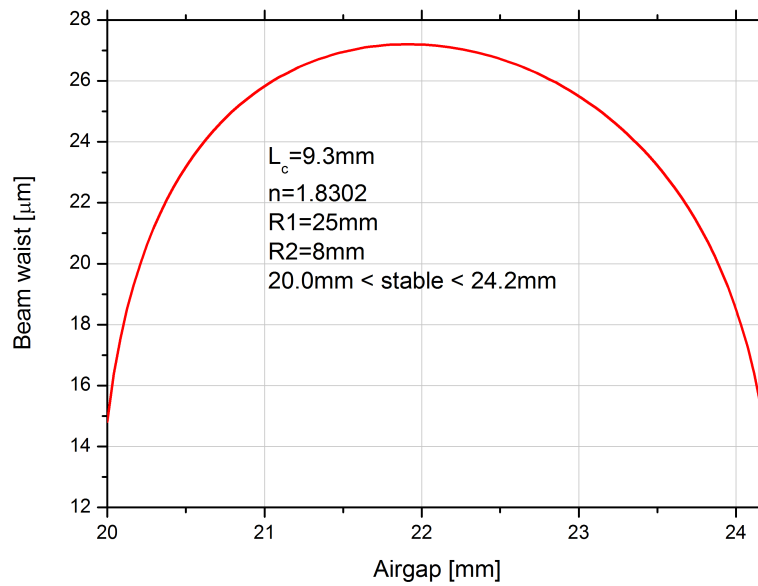


Figure 3.2. Radius of the SHG beam waist as a function of the optical cavity length, determined by the air gap between the coupling mirror and the AR-coated crystal facet. The cavity stability range extends from 20.0mm to 24.2mm . Parameters: crystal length: 9.30mm , $n(\text{PPKTP}, 1064\text{nm}) = 1.8306$, crystal RoC: 8mm , coupling mirror RoC: 25mm .

3.2.2 Temperature control

The achievement and maintenance of the crystal phase matching condition is made by a digital PID loop with frequency bandwidth of few Hz . The crystal heater is a peltier element [brand and model] while the temperature sensors is PTC sensor [brand and model]. One PTC output is used to close the control loop while the other is used to check the achieved temperature stability. With our design the achievable temperature stability is of the order of few mKRMS (see Fig. 3.3).

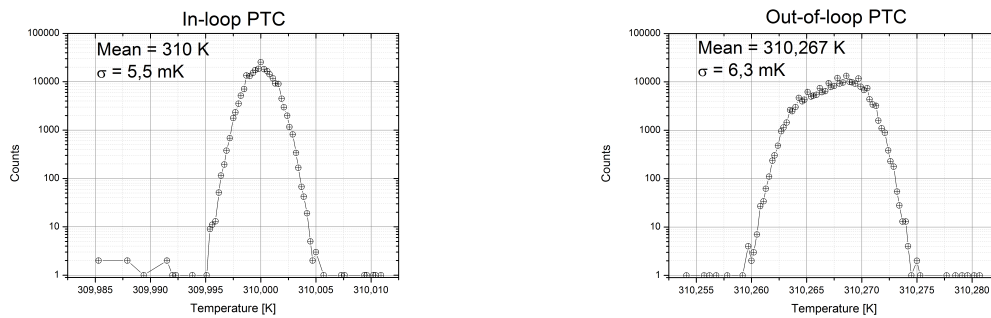


Figure 3.3. In loop and out of loop termistor histogram.

3.2.3 Mechanics

Fig. 3.5 (left side) shows an exploded of the SHG cavity. The base is made of alluminium. On that base there is a peltier cell with the heater upwards and above it there is an high conductivity

copper (OHFC) “L”. On this copper element, there are the two termistor that are mechanically attached to it with copper berillium springs (see Fig. 3.4). The results shown in Fig. 3.3 relate to a first version of the cavity that has been assembled with a completely dry set-up, avoiding the use of any kind of conductive pasta.

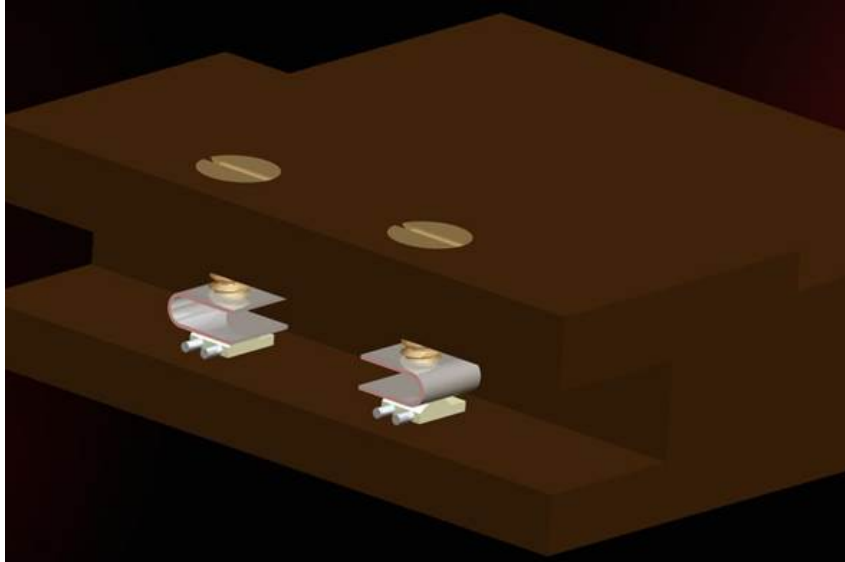


Figure 3.4. Dry assembly of the two termistor needed for the temperature control.

The NLC is hosted between the copper “L” and a macor “L”, held in place with four screws. To optimize the thermal contact between the crystal and the copper element, and to avoid a crack of the NLC, an indium foil ($100\mu m$) has been used.

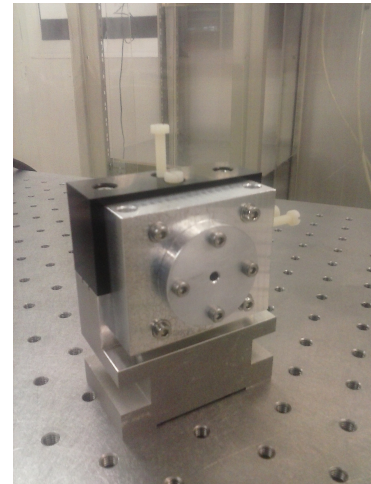
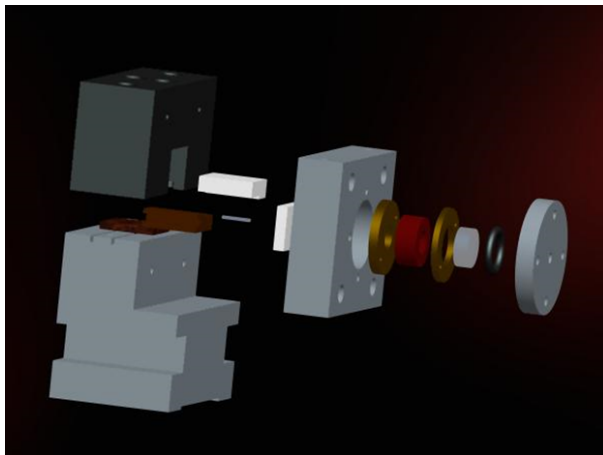


Figure 3.5. Exploded view of the SHG and image of a prototype.

3.2.4 PDH locking system for the SHG

The cavity length control loop is a standard Pound-Drever-Hall (PDH) loop.

3.2.5 IR to GREEN conversion

Preliminary measurements on the green conversion phase matching, obtained from the prototype, are shown in Fig. 3.6. The phase matching temperature is 305.2K and varies of about 0.5K depending on the frequency and on the power of the IR source.

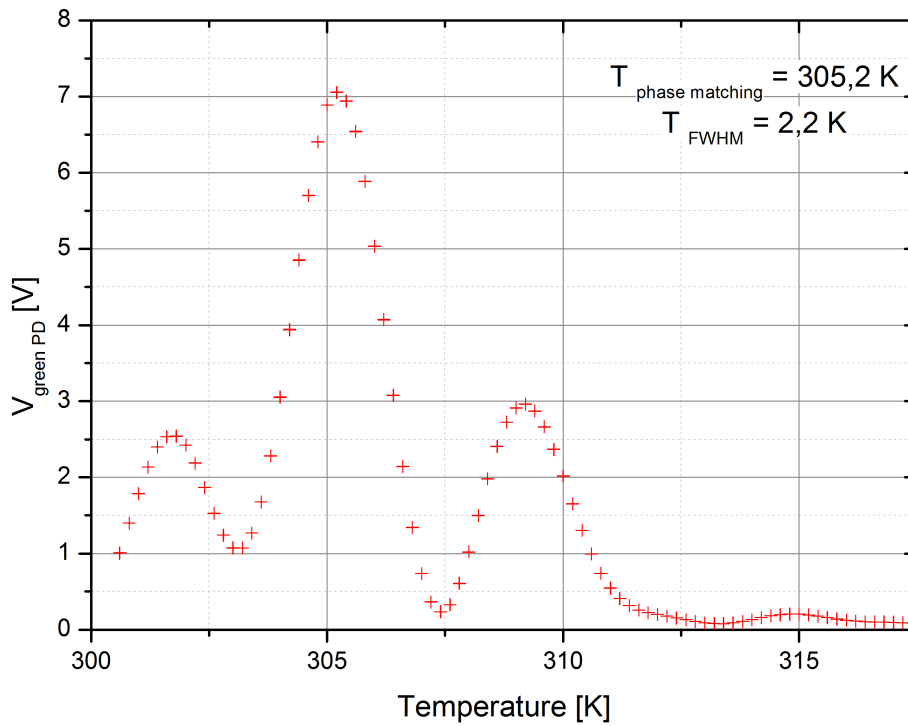


Figure 3.6. Quasi Phase Matching. Y axis needs to be calibrated.

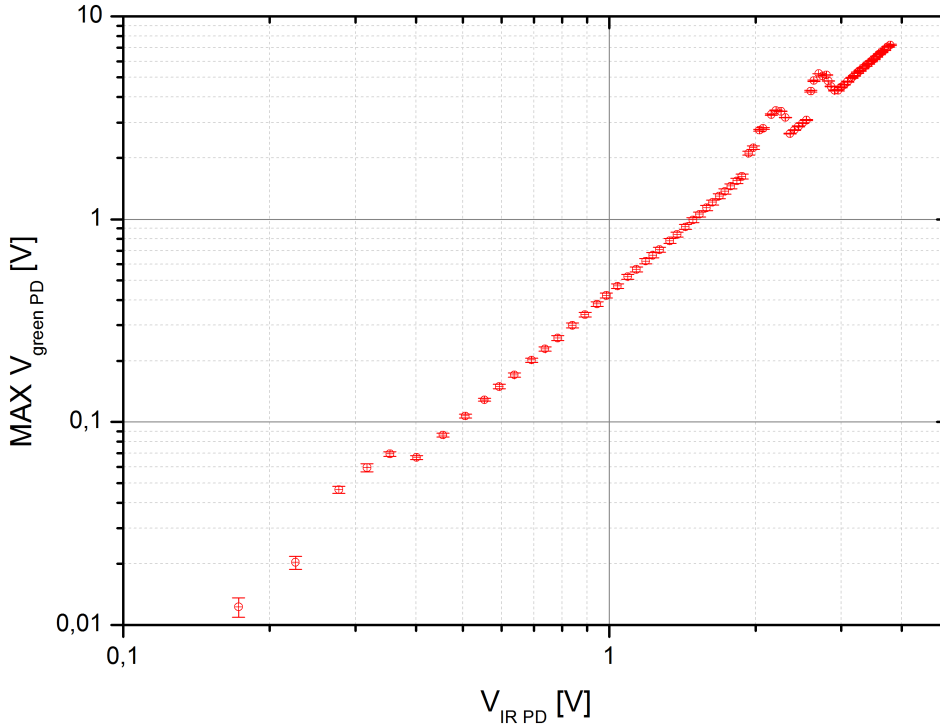


Figure 3.7. Example of IR to green conversion. Both axis needs to be calibrated.

3.3 Pump Beam Power Stabilization

Long-term squeezer operations requires the implementation of a pump power stabilization [7, 1]. The pump fluctuations cause a variation of the green light absorption in the OPO crystal and thus temperature fluctuations. The latest affect directly the squeezing degree by means of the non linear gain fluctuation but even the squeezing angle and the homodyne angle stability [6] by means of the cavity detuning that. Nevertheless the gain fluctuations due to the pump fluctuations results in a very weak squeezing value fluctuations, as shown in [6], where, considering realistic values for the OPO and of the homodyne detector parameters (i.e of the total intra-cavity losses, the escape efficiency, the propagation losses, the homodyne fringe visibility and efficiency) such that 9 dB of detected squeezing can be predicted, the estimate fluctuations due to a $\pm 10\%$ pump fluctuations are about ± 0.13 dB. More incisive are the effects of the detuning induced by the temperature fluctuations inside the non linear crystal. These lead to a refractive index change and thus to a loss of the phase matching conditions, since while DPH loop on the OPO assures the resonance of the beam used for the length stabilization (both if the OPO length is controlled in polarizations degeneracy conditions - i.e. by means of a beam with same frequency of the fundamental but orthogonal polarization - and if the length is stabilized on the pump resonance, like in the case of a doubly resonant OPO) the temperature change leads to a detuning of the fundamental beam inside the OPO. This detuning affects the coherent control scheme of the squeezing angle and the homodyne angle stabilization control too, so that it must be compensated by means of a fine, calibrated temperature control. Even if this is in principle realizable, the pump power stabilization results to be simpler and more precise, as experimentally observed in the LIGO-GEO experience [7, 1].

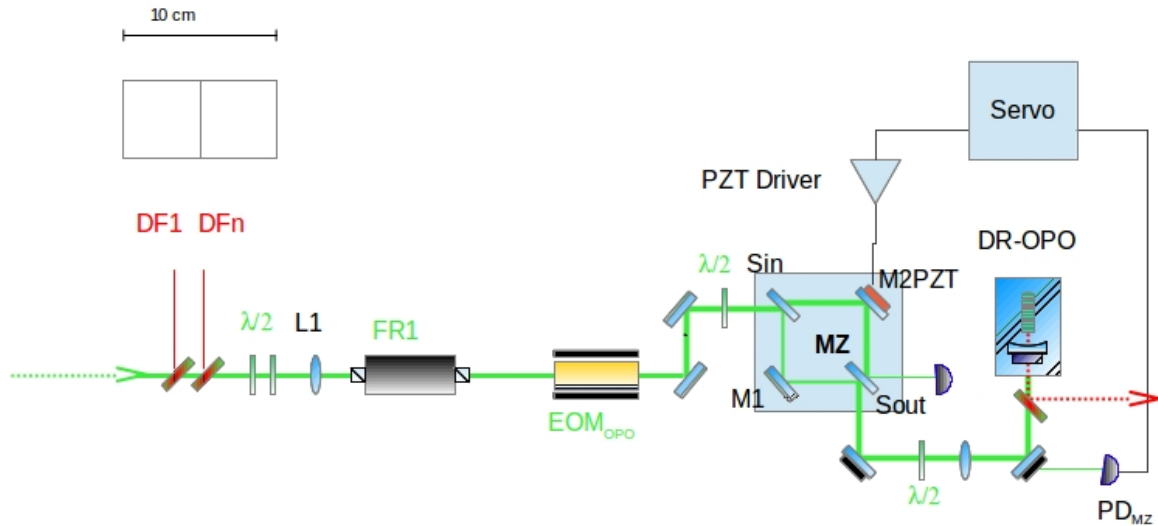


Figure 3.8. Sketch of the optical set-up and of the control loop for the OPO pump stabilization system based on a Mach-Zehnder.

A theoretical stability requirement can be easily calculated by means of the simple model presented in [6], taking into account all the above-mentioned effects and the attended parameters of our set-up. It results to be a **0.1** deviation of the pump beam power, since within this value the squeezing degree and angle does not significantly change.

3.3.1 System description

Following the GEO-LIGO experience, we realize a pump power stabilization system that does not rely on non-linear effect, based on a simple unbalanced Mach-Zehnder interferometer [6, 2, 13]. It results to be more efficient, simple and precise respect to the common noise eater based on the Pockels cells, since the absence of the non linear medium avoids the thermal effects that could cause aging and disease on the long period.

A simple sketch of the system principle of operation is shown in figure 3.8. The transmitted power tuning in the unbalanced Mach-Zehnder is provided by means of piezoelectric element (PZT) on one of the interferometer mirrors by changing the relative arms length. The monitoring and control of the squeezer pump power is made by extracting a small fraction of the 532 nm light close to the OPO input port by means of a photodetector. The detector signal is then compared with a reference voltage that sets the working point. The system allows to remove the long-term power pump fluctuations and to make possible a squeezing degree and squeezing angle stability. Moreover the possibility to tune the power provides adjustment after the first calibration of the squeezing values.

Our unbalanced interferometer has equal arms length and unbalanced beams power along each arm, so that the mean power outgoing from the two out-port is different. It is made of two UV fused silica beam samplers (S_{out} and S_{out} in the sketch of figure 3.8) with a transmittivity at 45° of 10 % for the p -polarization and of 1 % for the s -polarization. In these conditions the mean transmitted power at the two out-put ports of the interferometer are $P_{ort}^{mean} = 0.98$ and $P_{par}^{mean} = 0.02$ with a dynamic range of ± 0.02 for the p -polarization and $P_{ort}^{mean} = 0.82$ and $P_{par}^{mean} = 0.18$ with a dynamic range of ± 0.2 for the s -polarization. The other two mirrors along

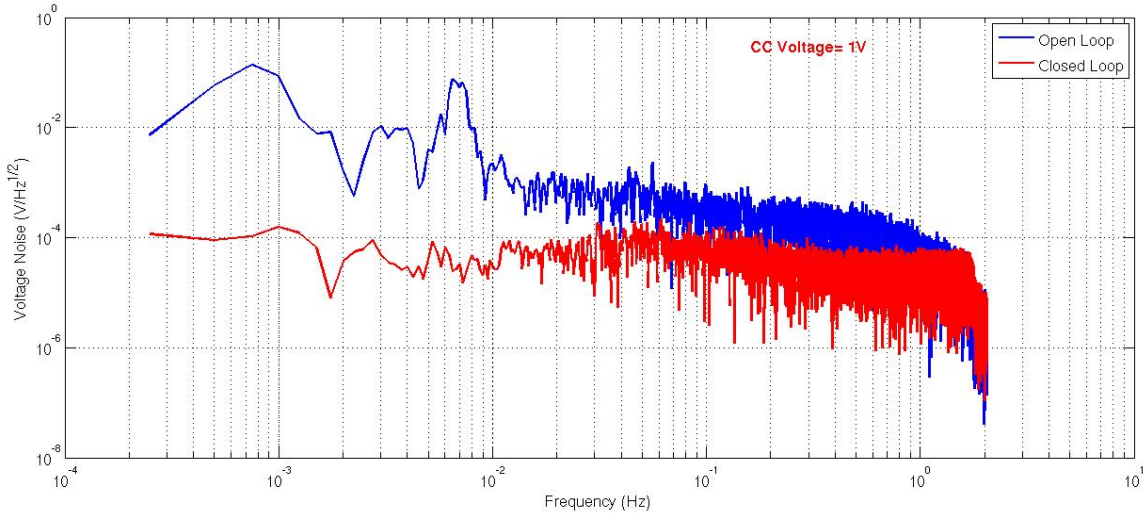


Figure 3.9. Spectrum of the detected output signal of the Mach-Zehnder power stabilization system. This preliminary test - done with a system prototype - shows a stability well below the required 1 %.

the interferometer arms, M_1 and M_2 , are HR mirrors with a reflectivity $R > 0.9999$ and a super-polished reflective surface with rms surface roughness $\sim 0.5 \text{ \AA}$ and a scratch/dig of 10/5. A $\lambda/2$ waveplate before the interferometer input port allows the polarization adjustment and thus the tuning of the mean transmitted power. The waveplate at the output along the pump beam path, re-adjusts the polarization. A first, rough alignment of the system can be done by means of an input beam steering. The piezoelectric, PZT on the mirror M_2 (see figure 3.8) is a compact, high-speed multi-axis tip/tilt and z-positioners, the PI S-310, that has a resonant frequency of $6.1 \pm 1.2 \text{ kHz}$ with a 1 inch fused silica mirrors. It allows the fine interferometer alignment, while the rough alignment can be performed by means of the precision adjustment screws on the M_1 mirror holder.

The unity gain frequency of the closed loop system is **1 kHz**.

The results of a preliminary prototype are already compliant with the specifications, as can be seen in the graphics of figure 3.9.

3.3.2 Mechanical design

The mechanical design of the Mach-Zehnder interferometer holder is shown in figure 3.10 The holders of the Mach-Zehnder mirrors are mounted on a square aluminum base with height 35.6 mm. The M_1 mirror holder is the Newport 9817-6 of the Stability™ series. It is a clean and low-outgassing mirror mount with an optics center height equal to 25.4 mm. An adapter, suitably designed, allows the mounting of the M_2 mirror fixed on the PZT on the same kind of holder. The beam sampler are fixed at 45° on the base by means of a single thin aluminum plate that assures their relative position and a center height of 1 inch. The center of the optics is in this way fixed at 61 mm. The whole mechanical system is designed to be vacuum compatible.

3.3.3 Electronic control loop

Figure 3.10. Mechanical design of the Mach-Zehnder interferometer holder.

MZ closed loop transfer function

Figure 3.11. Transfer function of the closed loop system.

3.4 OPO pre-Mode Cleaner Cavity

The *mode-cleaner* cavities (MC) have a crucial role in quantum optics experiments based on OPO/OPA sources and in particular in the squeezing experiments [15, 6, 14] thanks to their frequency and spatial filtering features. Spatially they reflect the mode higher than the TEM_{00} allowing the power concentration in the latest. In the frequency space they acts as low-pass filter for the laser amplitude and phase noise: outside the cavity linewidth, the amplitude noise of the injected laser field is attenuated with a single cavity-pole transfer function. In particular this feature has been demonstrated to be a crucial key to reach higher squeezing value since it filters the high frequency phase noise introduced by the Drever Pound Hall locking systems (DPH) by means of the RF modulation [14, 5, 12]. Furthermore a ring pre-MC acts as polarization filter [8].

3.4.1 532MC optical parameters

The pre-MC is a triangular cavity ring resonators with two plane input/output coupler mirrors and the third one plane-concave with $RoC = 1$ m. It has been designed performing a trade-off between the minimization of the astigmatism and the minimization of the backscattering [8], so that the incidence input angle has been chosen $\alpha = 43.88^\circ$, resulting in a incidence angle on the concave mirror $\theta = 2.25^\circ$. The cavity length is $L_{MC532} = 582.29$ mm. In the table 3.1 the cavity geometrical parameters are reported, included the stability factor, g .

	w_0 (μm)	w_{in} (μm)	w_{out} (μm)	w_{cc} (μm)	z_R (mm)	Gouy phase (π)	g
x	392.036	392.151	392.151	465.785	453.797	0.3625	0.6991
y	392.463	392.577	392.577	465.996	454.784	0.3631	0.7006

Table 3.1. Geometrical parameters of the 532MC. LEGENDA: w_0 beam waist size; w_{in} beam waist size on the input planar mirror; w_{out} beam waist size on the output planar mirror; w_{cc} beam waist size on the concave mirror; z_R Rayleigh parameter; g stability factor of the equivalent plane cavity.

All the mirrors will be super-polished and the reflectivity of the input and output coupler is $R = 0.995$, while the reflectivity of the rear concave mirror is $R = 0.9998$.

The resulting finesse is $\mathcal{F} = 614$, the linewidth $FWHM = 837.85$ kHz and the free spectral range $FSR = 514.85$ MHz

3.4.2 532MC mechanical design

The holder of the pre-MC is made of an INVAR bar with the mirrors mechanically fixed to it by means of aluminum holder, in order to avoid the mirrors coating contamination by means of the glue (figure 3.12). The invar holder has wedge-shaped lateral walls at 15° to allow to the eventually scattered photons on them to fast leave the cavity. The concave mirror holder hosts the PZT of the DPH locking system. The system is a sandwich of PZT, a aluminum ring, the mirror and a elastic viton ring hosted in a suitably trilled holder that is fixed on the main invar body by means of screws. The aluminum ring between the PZT and the mirror assure that no deformation on the center of the mirror surface can happen. All the system is vacuum compatible, having suitable hair holes where necessary.

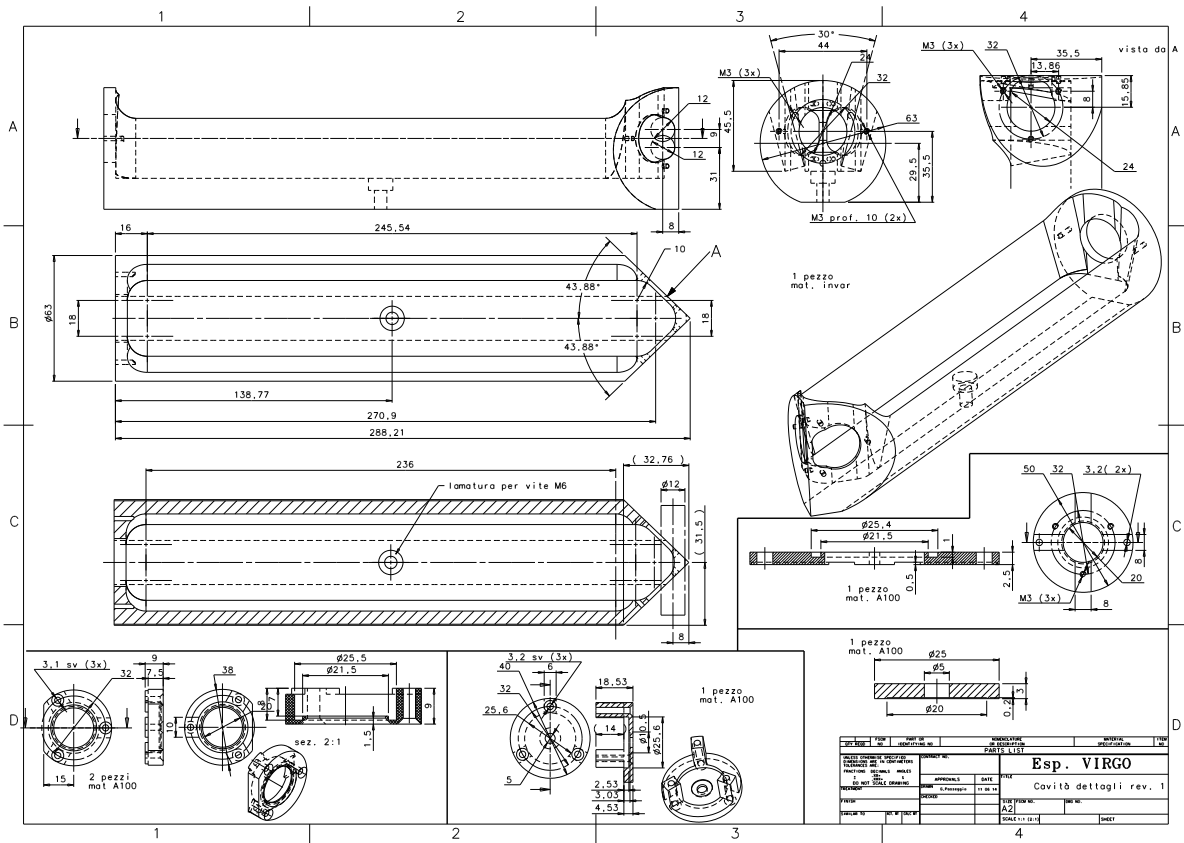


Figure 3.12. CAD design of the MC holder. N.B.: The concave mirror design is not the definitive.

3.4.3 532MC control system

Bibliography

- [1] J Aasi et al. “Enhanced sensitivity of the LIGO gravitational wave detector by using squeezed states of light”. In: *Nature Photonics* 7.8 (2013), pp. 613–619.
- [2] Simon Chelkowski. “Squeezed Light and Laser Interferometric Gravitational Wave Detectors”. Thesis. Von der Fakultät für Mathematik und Physik der Gottfried Wilhelm Leibniz Universität Hannover zur Erlangung des Grades, 2007.
- [3] Sheon Chua. “Quantum Enhancement of a 4km Laser Interferometer Gravitational-Wave Detector”. Thesis. The Australian National University, 2013.
- [4] A. Freise. *finesse (Frequency domain INterferomEter Simulation SoftwarE) 0.99.8*. URL: <http://www.gwoptics.org/finesse/>.
- [5] Alexander Franzen et al. “Experimental demonstration of continuous variable purification of squeezed states”. In: *Physical review letters* 97.15 (2006), p. 150505.
- [6] Aleksandr Khalaidovski. “Beyond the Quantum Limit. A squeezed-Light Laser in GEO 600”. Thesis. Von der Fakultät für Mathematik und Physik der Gottfried Wilhelm Leibniz Universität Hannover zur Erlangung des Grades, 2011.
- [7] LIGO Scientific Collaboration et al. “A gravitational wave observatory operating beyond the quantum shot-noise limit”. In: *Nature Physics* 7.12 (2011), pp. 962–965.
- [8] Fred Raab and Stan Whitcomb. “Estimation of special optical properties of a triangular ring cavity”. In: *LIGO T920004-00* (1992).
- [9] URL: <http://raicol.com/>.
- [10] Michael Stefszky et al. “An investigation of doubly-resonant optical parametric oscillators and nonlinear crystals for squeezing”. In: *Journal of Physics B: Atomic, Molecular and Optical Physics* 44.1 (2011), p. 015502.
- [11] Michael Steve Stefszky. “Generation and Detection of Low-Frequency Squeezing for Gravitational-Wave Detection”. Thesis. The Australian National University, 2012.
- [12] Yuishi Takeno et al. “Observation of 9 dB quadrature squeezing with improvement of phase stability in homodyne measurement”. In: *Optics Express* 15.7 (2007), pp. 4321–4327.
- [13] Henning Vahlbruch. “Squeezed Light for Gravitational Wave Astronomy”. Thesis. Von der Fakultät für Mathematik und Physik der Gottfried Wilhelm Leibniz Universität Hannover zur Erlangung des Grades, 2008.
- [14] Henning Vahlbruch et al. “Observation of squeezed light with 10-dB quantum-noise reduction”. In: *Physical review letters* 100.3 (2008), p. 033602.
- [15] B Willke et al. “Spatial and temporal filtering of a 10-W Nd: YAG laser with a Fabry–Perot ring-cavity premode cleaner”. In: *Optics letters* 23.21 (1998), pp. 1704–1706.